https://mathco.journals.pnu.ac.ir

Payame Noor University

**Control and Optimization in Applied Mathematics**

Volume 11, Issue 2, Summer-Autumn 2026, Pages 83–103

DOI:10.30473/coam.2026.77066.1388

OPEN ACCESS

Control and Optimization in Applied Mathematics

Research Article

# Optimization-Oriented Double Pre-Test Shrinkage Estimators for Pareto Reliability under Progressive Type-II Censoring and Precautionary Loss

**Omar J. A. Al-Qaragholi** ✉ **Alaa Khlaif Jiheel**

Department of Mathematics, College of Education for Pure Sciences, University of Thi-Qar, Nasiriyah, Iraq

**Article History**

*Received*: January 4, 2026
*Accepted*: April 2, 2026
*Available online*: May 21, 2026

**Abstract.** This paper develops and analyzes a class of double pre-test shrinkage estimators for the reliability function of the Pareto distribution under progressively Type-II censored samples. The proposed framework integrates a preliminary test of the shape parameter against a prior target value with shrinkage toward the corresponding prior reliability, producing four reliability estimators with both fixed and data-dependent shrinkage weights. Closed-form expressions are derived for the bias, bias ratio, risk functions under the Precautionary Loss Function (PLF), and relative risk with respect to the classical pooled estimator. Numerical results are obtained through direct evaluation of the derived analytical expressions—including one- and two-dimensional integrals and special functions—implemented in Python. Across a broad range of design settings and reliability levels, the proposed estimators consistently reduce PLF-risk and improve relative efficiency, with the most pronounced gains occurring when the prior ratio $\lambda = \theta_0/\theta$ is near unity. The estimation problem is further interpreted as an optimization problem under uncertainty, in which PLF-risk serves as the objective function and the design parameters—including the shrinkage weight, significance level, and stage sample sizes—define the feasible decision space.

**Keywords.** Double pre-test shrinkage estimation, Pareto reliability function, Progressive Type-II censoring, Precautionary loss function, Optimization under uncertainty.

**MSC.** 62N05; 90C90; 62F30.

**How to Cite**

Al-Qaragholi, O.J.A., Jiheel, A.Kh. (2026). "Optimization-oriented double pre-test shrinkage estimators for Pareto reliability under progressive Type-II censoring and precautionary loss". *Control and Optimization in Applied Mathematics*, 11(2), 83-103. https://doi.org/10.30473/coam.2026.77066.1388

✉Corresponding author. **E-mail:** omar_jabar@utq.edu.iq

## 1 Introduction

Reliability estimation is fundamental in engineering, quality control, and risk analysis, where decisions often depend on the probability that a component or system survives beyond a specified mission time. Heavy-tailed lifetime distributions arise naturally in many applications, including insurance, economics, and reliability under heterogeneous populations, and the Pareto distribution is a widely used model in this context [1, 4, 15]. In practice, lifetime experiments are frequently conducted under censoring because of time or cost constraints. Among the most flexible schemes is progressive Type-II censoring, which allows planned removals of surviving units at intermediate failure times and is widely used in modern reliability experimentation [6, 7, 15].

A key methodological objective is to improve estimation accuracy by incorporating prior or engineering information whenever such information is available. Shrinkage and pre-test ideas are classical tools for this purpose: shrinkage combines a conventional estimator with a prior target value, whereas preliminary pre-test procedures adapt the estimator according to whether the data are consistent with the target hypothesis [2, 3, 9, 14]. When data arise from multi-stage sampling, pooled and double-stage constructions can further stabilize inference, which is particularly valuable under censoring where effective sample sizes are reduced and estimation uncertainty is increased. Motivated by this setting, we develop a double pre-test structure that combines two-stage pooling with an explicit acceptance region and then applies shrinkage toward a prior target.

In addition to the estimator structure, the loss criterion used to evaluate reliability procedures should reflect the asymmetric consequences of estimation error in risk-sensitive settings. Classical symmetric criteria such as mean squared error treat over- and under-estimation similarly, which may be inadequate when underestimating risk, or overestimating reliability, is more costly in practice. The Precautionary Loss Function (PLF) provides a reliability-oriented alternative: it is scale-invariant and assigns a stronger penalty to harmful deviations, making it a natural choice for decision-making under uncertainty [12, 13].

**Research Gap and Novelty.** Despite the extensive literature on shrinkage and pre-test estimation, reliability results under progressive Type-II censoring have been developed mainly for other lifetime models and often under symmetric loss criteria [5, 8, 10]. For the Pareto model, related studies commonly emphasize estimation of the shape parameter itself or focus on alternative inferential settings, including Bayesian and prediction-based formulations [1, 11, 15], while analytical PLF-based risk comparisons for reliability estimators under progressively Type-II censored samples remain limited. Moreover, the specific combination of a double pre-test mechanism, based on two-stage pooling governed by an acceptance region, with shrinkage toward a prior target has received only limited attention in closely related models such as Burr XII and Exponential settings [5, 13] and, to the best of our knowledge, has not been developed in this specific combination for the Pareto reliability function within a PLF framework. This paper addresses these gaps by providing a unified construction and a full analytical-numerical performance assessment tailored to Pareto reliability under progressive Type-II censoring.

**Optimization Perspective.** Beyond its statistical formulation, the present work can also be viewed as an optimization problem under uncertainty. In particular, the proposed double pre-test shrinkage estimators are evaluated through the minimization of the PLF-risk over admissible shrinkage and design choices, subject to the structural constraints imposed by the acceptance region and the two-stage sampling scheme. The fixed-weight estimator selects a constant shrinkage weight to control risk at a specified prior ratio $\lambda = \theta_0/\theta$, whereas the data-dependent estimators employ adaptive weighting rules driven by the observed test statistic, thereby yielding a constrained data-guided estimator design. In this setting, the relative risk criterion serves as an objective function for comparing competing reliability procedures, while the closed-form PLF-risk expressions derived later in the paper provide an analytical basis for optimization over the design parameters, including the shrinkage weight, significance level, and stage sample sizes.

**Main contributions.** The main contributions of this work are as follows: (i) We propose four double pre-test shrinkage estimators for the Pareto reliability function, combining a preliminary test on the shape parameter with shrinkage toward a prior target value $\theta_0$, or equivalently a prior ratio $\lambda = \theta_0/\theta$. (ii) We derive closed-form analytical expressions for the bias and bias ratio of the proposed estimators, together with PLF-risk functions and relative risk measures compared with the classical pooled estimator, expressed in terms of standard special functions, including the regularized incomplete gamma function and the modified Bessel function of the second kind. (iii) For reproducibility, all numerical results are produced via direct numerical evaluation of the derived analytical expressions, implemented in Python, rather than by Monte Carlo simulation. (iv) A comprehensive numerical study examines performance across sample allocations, significance levels, and prior ratios, highlighting the strongest improvements near $\lambda \approx 1$, where the prior is well aligned with the true parameter. This analysis also clarifies how the design parameters influence PLF-risk and hence supports an optimization-oriented interpretation of the estimator construction.

The remainder of the paper is organized as follows. Section 2 presents the model and the proposed double pre-test shrinkage reliability estimators under progressive Type-II censoring. Section 3 derives the bias ratio, PLF-risk functions, and relative risk measures. Section 4 reports the numerical results, including graphical and tabular summaries, from the analytical evaluation and discusses their implications from both reliability and design-optimization perspectives. Section 5 concludes the paper with practical recommendations.

## 2 Model and Proposed Estimators

Consider a progressively Type-II censored sample from the Pareto distribution with shape parameter $\theta > 0$ and reliability function

$$R(t;\theta) = P(T > t) = t^{-\theta}, \qquad t > 1. \tag{1}$$

Let

$$X_{1:m:n} < X_{2:m:n} < \cdots < X_{m:m:n},$$

denote the observed progressively Type-II censored order statistics obtained from an initial sample of size $n$, under the censoring scheme

$$(R_1, R_2, \ldots, R_m),$$

where $R_i$ units are removed at the time of the $i$th observed failure, $i = 1, 2, \ldots, m$, and

$$n = m + \sum_{i=1}^{m} R_i.$$

For the Pareto model considered in this paper, the reliability function at a specified mission time $t > 1$ depends only on the shape parameter $\theta$, as given in (1). Accordingly, estimation of the reliability function reduces to estimation of $\theta$ under progressive Type-II censoring.

To construct the proposed class of estimators, we consider two independent progressively Type-II censored samples from the same Pareto model, corresponding to the first and second stages of sampling. Let $\hat{\theta}_1$ and $\hat{\theta}_2$ denote the stage-wise estimators of $\theta$, and let $\theta_0$ be a prior target value for the shape parameter. The associated prior reliability is

$$R_0(t) = R(t;\theta_0) = t^{-\theta_0}. \tag{2}$$

A preliminary test is first performed for the hypothesis

$$H_0 : \theta = \theta_0 \qquad \text{against} \qquad H_1 : \theta \neq \theta_0. \tag{3}$$

Let $\tau$ denote the corresponding test statistic, and let

$$\mathcal{C} = \{r_1 < \tau < r_2\}, \tag{4}$$

be the acceptance region of the test at significance level $\alpha$, where $r_1$ and $r_2$ are the lower and upper critical values, respectively.

The proposed double pre-test construction combines two-stage pooling with shrinkage toward the prior target. When the event $\mathcal{C}$ occurs, shrinkage is applied toward $R_0(t)$; otherwise, the classical pooled rule is used. Let $\hat{R}_1(t) = t^{-\hat{\theta}_1}$ and $\hat{R}_2(t) = t^{-\hat{\theta}_2}$ denote the stage-wise reliability estimators. Then the classical pooled estimator is defined by

$$\tilde{R}_{cd}(t) = \frac{m_1\hat{R}_1(t) + m_2\hat{R}_2(t)}{m_1 + m_2}. \tag{5}$$

Using this construction, we define four double pre-test shrinkage estimators. The first estimator uses a fixed shrinkage weight $k_1 \in (0, 1)$:

$$\tilde{R}_{\text{dsh1}}(t) = \begin{cases} k_1\hat{R}_1(t) + (1 - k_1)R_0(t), & \tau \in \mathcal{C}, \\ \tilde{R}_{cd}(t), & \tau \notin \mathcal{C}. \end{cases} \tag{6}$$

**Remark 1.** The fixed shrinkage weight $k_1$ can be chosen to minimize the PLF-risk at a target prior ratio $\lambda_0$, yielding an optimal fixed-weight design. In the numerical study we consider $k_1 \in \{0.1, 0.5\}$ as representative values spanning strong and moderate shrinkage.

The second estimator uses the data-independent choice $k_2 = \alpha^2$:

$$\tilde{R}_{\text{dsh2}}(t) = \begin{cases} k_2\hat{R}_1(t) + (1 - k_2)R_0(t), & \tau \in \mathcal{C}, \\ \tilde{R}_{cd}(t), & \tau \notin \mathcal{C}. \end{cases} \tag{7}$$

The third estimator employs the adaptive weight

$$k_3 = \frac{\tau}{r_1 + r_2}, \tag{8}$$

which yields

$$\tilde{R}_{\text{dsh3}}(t) = \begin{cases} k_3\hat{R}_1(t) + (1 - k_3)R_0(t), & \tau \in \mathcal{C}, \\ \tilde{R}_{cd}(t), & \tau \notin \mathcal{C}. \end{cases} \tag{9}$$

Finally, the fourth estimator uses the squared adaptive weight

$$k_4 = k_3^2, \tag{10}$$

and is defined by

$$\tilde{R}_{\text{dsh4}}(t) = \begin{cases} k_4\hat{R}_1(t) + (1 - k_4)R_0(t), & \tau \in \mathcal{C}, \\ \tilde{R}_{cd}(t), & \tau \notin \mathcal{C}. \end{cases} \tag{11}$$

Table 1 provides a concise comparison of the four proposed estimators in terms of their shrinkage weight, weight type, and the conditions under which each is expected to perform best.

The above construction provides a unified framework for comparing fixed and adaptive shrinkage rules under progressive Type-II censoring. In the next section, analytical expressions for the bias ratio, PLF-risk, and relative risk of the proposed estimators are derived.

**Table 1:** Summary comparison of the four proposed double pre-test shrinkage estimators.

| Estimator | Shrinkage weight | Type | Recommended when |
|---|---|---|---|
| $\tilde{R}_{\text{dsh1}}$ | $k_1 \in (0,1)$, fixed | Fixed | Prior information is reliable and $\lambda \approx 1$; $k_1$ is tunable to control the risk–bias trade-off |
| $\tilde{R}_{\text{dsh2}}$ | $k_2 = \alpha^2$, fixed | Fixed | A small significance level $\alpha$ is used, yielding strong shrinkage toward $R_0$ |
| $\tilde{R}_{\text{dsh3}}$ | $k_3 = \tau/(r_1 + r_2)$, adaptive | Data-dependent | Moderate prior uncertainty; weight adapts linearly to the observed test statistic |
| $\tilde{R}_{\text{dsh4}}$ | $k_4 = k_3^2$, adaptive | Data-dependent | Stronger shrinkage than $\tilde{R}_{\text{dsh3}}$ is desired; weight shrinks quadratically |

## 3 Bias Ratio and PLF-Risk Derivations

### 3.1 Bias and Bias Ratio

Throughout this section, we fix a mission time $t > 1$ and write

$$R(t;\theta) = t^{-\theta}, \qquad \lambda = \frac{\theta_0}{\theta}. \tag{12}$$

For any estimator $\tilde{R}$ of $R(t;\theta)$, define

$$(\tilde{R}) = \mathbb{E}(\tilde{R}) - R(t;\theta), \qquad (\tilde{R}) = \frac{(\tilde{R})}{R(t;\theta)}. \tag{13}$$

Let $\hat{\theta}_1$ and $\hat{\theta}_2$ be the independent stage-wise MLEs based on $m_1$ and $m_2$ observed failures, with densities $f_1(\hat{\theta}_1)$ and $f_2(\hat{\theta}_2)$ given in Section 2. The acceptance region is $\mathcal{C} = \{r_1 < \tau < r_2\}$, where $\tau = 2m_1\theta_0/\hat{\theta}_1$, and hence $\mathcal{C}$ depends on $\hat{\theta}_1$ only.

**Bias ratio of $\tilde{R}_{\text{dsh1}}$ and $\tilde{R}_{\text{dsh2}}$**

**Bias definition and decomposition over $\mathcal{C}$.** For $\tilde{R}_{\text{dsh1}}$ defined in (6),

$$(\tilde{R}_{\text{dsh1}}) = \mathbb{E}(\tilde{R}_{\text{dsh1}}) - t^{-\theta}. \tag{14}$$

Its expectation is decomposed over $\mathcal{C}$ and $\overline{\mathcal{C}}$ as

$$\begin{aligned}\mathbb{E}(\tilde{R}_{\text{dsh1}}) = &\int_0^\infty \int_{\mathcal{C}} \left[k_1\hat{R}_1 + (1-k_1)R_0\right] f_1(\hat{\theta}_1) f_2(\hat{\theta}_2)\, d\hat{\theta}_1\, d\hat{\theta}_2 \\ &+ \int_0^\infty \int_{\overline{\mathcal{C}}} \left[\tfrac{m_1\hat{R}_1 + m_2\hat{R}_2}{m_1+m_2}\right] f_1(\hat{\theta}_1) f_2(\hat{\theta}_2)\, d\hat{\theta}_1\, d\hat{\theta}_2,\end{aligned} \tag{15}$$

where $\hat{R}_i = t^{-\hat{\theta}_i}$ $(i = 1, 2)$ and $R_0 = t^{-\theta_0}$. Using

$$\int_{\overline{\mathcal{C}}}(\cdot) = \int_{(0,\infty)^2}(\cdot) - \int_{\mathcal{C}}(\cdot),$$

together with the independence of $(\hat{\theta}_1, \hat{\theta}_2)$, the terms reduce to one-dimensional $\mathcal{C}$-components in $\hat{\theta}_1$ multiplied by full-range components in $\hat{\theta}_2$.

**Change of variables on the $\mathcal{C}$-part.** Introduce

$$W = \frac{m_1\theta}{\hat{\theta}_1}, \qquad M = \frac{m_2\theta}{\hat{\theta}_2}, \qquad a_1 = m_1\theta \ln t, \qquad a_2 = m_2\theta \ln t, \tag{16}$$

so that $\hat{R}_1 = \exp(-a_1/W)$ and $\hat{R}_2 = \exp(-a_2/M)$, and

$$f_1(\hat{\theta}_1)\, d\hat{\theta}_1 = \frac{1}{\Gamma(m_1)} W^{m_1-1} e^{-W}\, dW, \qquad f_2(\hat{\theta}_2)\, d\hat{\theta}_2 = \frac{1}{\Gamma(m_2)} M^{m_2-1} e^{-M}\, dM. \tag{17}$$

Moreover, since $\tau = 2m_1\theta_0/\hat{\theta}_1 = 2\lambda W$, the region $\mathcal{C}$ becomes

$$\mathcal{C}^\star : \; r_1' < W < r_2', \qquad r_i' = \frac{r_i}{2\lambda}, \quad i = 1, 2. \tag{18}$$

**Special functions.** Define

$$I(u, m) = \frac{1}{\Gamma(m)} \int_0^u s^{m-1} e^{-s}\, ds, \tag{19}$$

and use

$$\int_0^\infty s^{\nu-1} \exp\Big(-s - \frac{a}{s}\Big)\, ds = 2a^{\nu/2} K_\nu\big(2\sqrt{a}\big), \qquad a > 0, \tag{20}$$

with $K_{-\nu} = K_\nu$. Then

$$\int_{\mathcal{C}} f_1(\hat{\theta}_1)\, d\hat{\theta}_1 = I(r_2', m_1) - I(r_1', m_1), \tag{21}$$

and

$$\mathbb{E}(\hat{R}_i) = \frac{2a_i^{m_i/2}}{\Gamma(m_i)} K_{m_i}\big(2\sqrt{a_i}\big), \qquad i = 1, 2. \tag{22}$$

**Final closed form.** After substitution and simplification, the bias is

$$\begin{aligned}
(\tilde{R}_{\text{dsh1}}) = {} & \Big(k_1 - \frac{m_1}{m_1+m_2}\Big) \frac{1}{\Gamma(m_1)} \int_{r_1'}^{r_2'} W^{m_1-1} \exp\Big(-W - \frac{a_1}{W}\Big)\, dW \\
& + (1-k_1)\, t^{-\lambda\theta} \Big[ I(r_2', m_1) - I(r_1', m_1) \Big] \\
& + \frac{m_1}{m_1+m_2} \frac{2a_1^{m_1/2}}{\Gamma(m_1)} K_{m_1}\big(2\sqrt{a_1}\big) + \frac{m_2}{m_1+m_2} \frac{2a_2^{m_2/2}}{\Gamma(m_2)} K_{m_2}\big(2\sqrt{a_2}\big) \\
& - \frac{m_2}{m_1+m_2} \Big[ I(r_2', m_1) - I(r_1', m_1) \Big] \frac{2a_2^{m_2/2}}{\Gamma(m_2)} K_{m_2}\big(2\sqrt{a_2}\big) - t^{-\theta}.
\end{aligned} \tag{23}$$

Hence,

$$(\tilde{R}_{\text{dsh1}}) = \frac{(\tilde{R}_{\text{dsh1}})}{t^{-\theta}}. \tag{24}$$

For $\tilde{R}_{\text{dsh2}}$ defined in (7), the derivation is identical, and we only replace $k_1$ by $k_2$:

$$(\tilde{R}_{\text{dsh2}}) = (\tilde{R}_{\text{dsh1}})\big|_{k_1 \to k_2}, \qquad (\tilde{R}_{\text{dsh2}}) = \frac{(\tilde{R}_{\text{dsh2}})}{t^{-\theta}}. \tag{25}$$

**Bias ratio of $\tilde{R}_{\text{dsh3}}$**

**Bias definition and same decomposition.** For $\tilde{R}_{\text{dsh3}}$ defined in (9),

$$(\tilde{R}_{\text{dsh3}}) = \mathbb{E}(\tilde{R}_{\text{dsh3}}) - t^{-\theta}. \tag{26}$$

We use exactly the same decomposition over $\mathcal{C}$ and $\overline{\mathcal{C}}$ and the same change of variables $W, M$ as above.

**The only new point.** On $\mathcal{C}^\star$ we must substitute

$$k_3 = \frac{\tau}{r_1 + r_2} = \frac{2\lambda W}{r_1 + r_2} \qquad (W \in \mathcal{C}^\star). \tag{27}$$

This introduces the additional $\mathcal{C}^\star$ component

$$\frac{1}{\Gamma(m_1)} \int_{r_1'}^{r_2'} W^{m_1} e^{-W}\, dW = m_1 \Big[ I(r_2', m_1 + 1) - I(r_1', m_1 + 1) \Big]. \tag{28}$$

**Final closed form.** After substitution and simplification, the bias becomes

$$\begin{aligned}
(\tilde{R}_{\text{dsh3}}) = {} & \frac{2\lambda}{r_1 + r_2} \cdot \frac{1}{\Gamma(m_1)} \int_{r_1'}^{r_2'} W^{m_1} \exp\Big( - W - \frac{a_1}{W} \Big)\, dW \\
& + t^{-\lambda\theta} \left[ \Big( I(r_2', m_1) - I(r_1', m_1) \Big) - \frac{2\lambda m_1}{r_1 + r_2} \Big( I(r_2', m_1 + 1) - I(r_1', m_1 + 1) \Big) \right] \\
& + \frac{m_1}{m_1 + m_2} \frac{2a_1^{m_1/2}}{\Gamma(m_1)} K_{m_1}\big(2\sqrt{a_1}\big) + \frac{m_2}{m_1 + m_2} \frac{2a_2^{m_2/2}}{\Gamma(m_2)} K_{m_2}\big(2\sqrt{a_2}\big) \\
& - \frac{m_1}{m_1 + m_2} \frac{1}{\Gamma(m_1)} \int_{r_1'}^{r_2'} W^{m_1 - 1} \exp\Big( - W - \frac{a_1}{W} \Big)\, dW \\
& - \frac{m_2}{m_1 + m_2} \Big( I(r_2', m_1) - I(r_1', m_1) \Big) \frac{2a_2^{m_2/2}}{\Gamma(m_2)} K_{m_2}\big(2\sqrt{a_2}\big) - t^{-\theta}.
\end{aligned} \tag{29}$$

Hence,

$$(\tilde{R}_{\text{dsh3}}) = \frac{(\tilde{R}_{\text{dsh3}})}{t^{-\theta}}. \tag{30}$$

**Bias ratio of $\tilde{R}_{\text{dsh4}}$**

**Bias definition and same decomposition.** For $\tilde{R}_{\text{dsh4}}$ defined in (11),

$$(\tilde{R}_{\text{dsh4}}) = \mathbb{E}(\tilde{R}_{\text{dsh4}}) - t^{-\theta}. \tag{31}$$

We proceed exactly as in the previous cases.

**Substitute $k_4$ on $\mathcal{C}^\star$.** On $\mathcal{C}^\star$ we substitute

$$k_4 = k_3^2 = \Big( \frac{2\lambda W}{r_1 + r_2} \Big)^2 \qquad (W \in \mathcal{C}^\star), \tag{32}$$

which introduces

$$\frac{1}{\Gamma(m_1)} \int_{r_1'}^{r_2'} W^{m_1 + 1} e^{-W}\, dW = m_1(m_1 + 1) \Big[ I(r_2', m_1 + 2) - I(r_1', m_1 + 2) \Big]. \tag{33}$$

**Final closed form.** After substitution and simplification,

$$
\begin{aligned}
(\tilde{R}_{\text{dsh4}}) = &\Big(\frac{2\lambda}{r_1+r_2}\Big)^2 \frac{1}{\Gamma(m_1)} \int_{r_1'}^{r_2'} W^{m_1+1} \exp\Big(-W-\frac{a_1}{W}\Big)\, dW \\
&+ t^{-\lambda\theta}\Bigg[\Big(I(r_2',m_1)-I(r_1',m_1)\Big) - \Big(\frac{2\lambda}{r_1+r_2}\Big)^2 m_1(m_1+1)\Big(I(r_2',m_1+2) \\
&- I(r_1',m_1+2)\Big)\Bigg] + \frac{m_1}{m_1+m_2}\frac{2a_1^{m_1/2}}{\Gamma(m_1)} K_{m_1}\big(2\sqrt{a_1}\big) \\
&+ \frac{m_2}{m_1+m_2}\frac{2a_2^{m_2/2}}{\Gamma(m_2)} K_{m_2}\big(2\sqrt{a_2}\big) \\
&- \frac{m_1}{m_1+m_2}\frac{1}{\Gamma(m_1)} \int_{r_1'}^{r_2'} W^{m_1-1} \exp\Big(-W-\frac{a_1}{W}\Big)\, dW \\
&- \frac{m_2}{m_1+m_2}\Big(I(r_2',m_1)-I(r_1',m_1)\Big)\frac{2a_2^{m_2/2}}{\Gamma(m_2)} K_{m_2}\big(2\sqrt{a_2}\big) - t^{-\theta}.
\end{aligned}
\tag{34}
$$

Therefore,

$$
(\tilde{R}_{\text{dsh4}}) = \frac{(\tilde{R}_{\text{dsh4}})}{t^{-\theta}}. \tag{35}
$$

### 3.2 PLF-risk and Relative Risk

Throughout this subsection, we fix a mission time $t > 1$ and write

$$
R(t;\theta) = t^{-\theta}, \qquad \lambda = \frac{\theta_0}{\theta}, \qquad a_1 = m_1\theta \ln t, \qquad a_2 = m_2\theta \ln t. \tag{36}
$$

Under the Precautionary Loss Function (PLF), the loss of a positive estimator $\tilde{R}$ of $R(t;\theta)$ is

$$
L(\tilde{R}, R) = \frac{\tilde{R}}{R(t;\theta)} + \frac{R(t;\theta)}{\tilde{R}} - 2, \qquad \tilde{R} > 0, \tag{37}
$$

and the corresponding PLF-risk is

$$
\mathcal{R}(\tilde{R} \mid \text{PLF}) = \mathbb{E}\Big[L(\tilde{R}, R)\Big]. \tag{38}
$$

Since $(\hat{\theta}_1, \hat{\theta}_2)$ are independent with densities $f_1(\hat{\theta}_1)$ and $f_2(\hat{\theta}_2)$ introduced in Section 2, the risk can be written explicitly as the double integral

$$
\mathcal{R}(\tilde{R} \mid \text{PLF}) = \int_0^\infty \int_0^\infty \left[\frac{\tilde{R}}{t^{-\theta}} + \frac{t^{-\theta}}{\tilde{R}} - 2\right] f_1(\hat{\theta}_1) f_2(\hat{\theta}_2)\, d\hat{\theta}_1\, d\hat{\theta}_2. \tag{39}
$$

**Benchmark estimator.** Recall the classical pooled reliability estimator

$$
\tilde{R}_{cd} = \frac{m_1\hat{R}_1 + m_2\hat{R}_2}{m_1+m_2}, \qquad \hat{R}_i = t^{-\hat{\theta}_i}, \quad i = 1, 2. \tag{40}
$$

**Decomposition over $\mathcal{C}$ and $\overline{\mathcal{C}}$.** For each proposed estimator $\tilde{R}_{\text{dsh}j}$, the definition is piecewise in terms of the acceptance region $\mathcal{C} = \{r_1 < \tau < r_2\}$, where $\tau = 2m_1\theta_0/\hat{\theta}_1$. Hence, the risk splits as

$$
\begin{aligned}
\mathcal{R}(\tilde{R}_{\text{dsh}j} \mid \text{PLF}) = &\int_0^\infty \int_{\mathcal{C}} \left[\frac{\tilde{R}_{\text{dsh}j}}{t^{-\theta}} + \frac{t^{-\theta}}{\tilde{R}_{\text{dsh}j}} - 2\right] f_1(\hat{\theta}_1) f_2(\hat{\theta}_2)\, d\hat{\theta}_1\, d\hat{\theta}_2 \\
&+ \int_0^\infty \int_{\overline{\mathcal{C}}} \left[\frac{\tilde{R}_{cd}}{t^{-\theta}} + \frac{t^{-\theta}}{\tilde{R}_{cd}} - 2\right] f_1(\hat{\theta}_1) f_2(\hat{\theta}_2)\, d\hat{\theta}_1\, d\hat{\theta}_2.
\end{aligned}
\tag{41}
$$

Using

$$\int_{\overline{\mathcal{C}}}(\cdot) = \int_{(0,\infty)^2}(\cdot) - \int_{\mathcal{C}}(\cdot),$$

we obtain the standard three-term form

$$\begin{aligned}\mathcal{R}(\tilde{R}_{\text{dsh}j} \mid \text{PLF}) = &\int_0^\infty \int_{\mathcal{C}} \left[\frac{\tilde{R}_{\text{dsh}j}}{t^{-\theta}} + \frac{t^{-\theta}}{\tilde{R}_{\text{dsh}j}} - 2\right] f_1 f_2 \, d\hat{\theta}_1 \, d\hat{\theta}_2 \\ &+ \int_0^\infty \int_0^\infty \left[\frac{\tilde{R}_{cd}}{t^{-\theta}} + \frac{t^{-\theta}}{\tilde{R}_{cd}} - 2\right] f_1 f_2 \, d\hat{\theta}_1 \, d\hat{\theta}_2 \\ &- \int_0^\infty \int_{\mathcal{C}} \left[\frac{\tilde{R}_{cd}}{t^{-\theta}} + \frac{t^{-\theta}}{\tilde{R}_{cd}} - 2\right] f_1 f_2 \, d\hat{\theta}_1 \, d\hat{\theta}_2,\end{aligned} \tag{42}$$

where $f_i = f_i(\hat{\theta}_i)$.

**Change of variables and acceptance region.** Introduce

$$W = \frac{m_1\theta}{\hat{\theta}_1}, \qquad M = \frac{m_2\theta}{\hat{\theta}_2}, \tag{43}$$

so that $\hat{R}_1 = \exp(-a_1/W)$ and $\hat{R}_2 = \exp(-a_2/M)$, and

$$f_1(\hat{\theta}_1)\, d\hat{\theta}_1 = \frac{1}{\Gamma(m_1)} W^{m_1-1} e^{-W}\, dW, \qquad f_2(\hat{\theta}_2)\, d\hat{\theta}_2 = \frac{1}{\Gamma(m_2)} M^{m_2-1} e^{-M}\, dM. \tag{44}$$

Moreover, since $\tau = 2m_1\theta_0/\hat{\theta}_1 = 2\lambda W$, the acceptance region becomes

$$\mathcal{C}^\star : \; r_1' < W < r_2', \qquad r_i' = \frac{r_i}{2\lambda}, \quad i = 1, 2. \tag{45}$$

We also use

$$I(u, m) = \frac{1}{\Gamma(m)} \int_0^u s^{m-1} e^{-s}\, ds, \tag{46}$$

and the Bessel identity

$$\int_0^\infty s^{\nu-1} \exp\Big(-s - \frac{a}{s}\Big)\, ds = 2a^{\nu/2} K_{-\nu}\big(2\sqrt{a}\big), \qquad a > 0, \tag{47}$$

with $K_{-\nu} = K_\nu$.

**PLF-risk of $\tilde{R}_{\text{dsh1}}$ and $\tilde{R}_{\text{dsh2}}$**

On $\mathcal{C}$, the estimator $\tilde{R}_{\text{dsh1}}$ uses $k_1\hat{R}_1 + (1-k_1)R_0$, while outside $\mathcal{C}$ it coincides with $\tilde{R}_{cd}$. Hence, in (42), the first integral over $\mathcal{C}$ becomes

$$\int_0^\infty \int_{\mathcal{C}} \left[t^\theta\big(k_1\hat{R}_1 + (1-k_1)R_0\big) + \frac{t^{-\theta}}{k_1\hat{R}_1 + (1-k_1)R_0} - 2\right] f_1 f_2 \, d\hat{\theta}_1 \, d\hat{\theta}_2,$$

which reduces to a one-dimensional $W$-integral over $\mathcal{C}^\star$ after the change of variables. The second and third terms in (42) are the full-space pooled risk and its $\mathcal{C}$-portion, which yield the Bessel and double-integral terms shown in the final expressions.

For $\tilde{R}_{\text{dsh2}}$, the derivation is identical, and we only replace $k_1$ by $k_2$.

The explicit closed form for $\tilde{R}_{\text{dsh1}}$ is:

$$\begin{aligned}\mathcal{R}(\tilde{R}_{\text{dsh1}} \mid \text{PLF}) = \frac{1}{\Gamma(m_1)} \int_{r_1'}^{r_2'} \Bigg[ & k_1\, t^{\theta} \exp\Big( -\frac{a_1}{W} \Big) + (1-k_1)\, t^{-(\lambda-1)\theta} \\ & + \frac{t^{-\theta}}{k_1 \exp(-a_1/W) + (1-k_1) t^{-\lambda\theta}} - 2 \Bigg] W^{m_1-1} e^{-W}\, dW \\ & + \frac{2m_1}{m_1+m_2} \frac{t^{\theta} a_1^{m_1/2}}{\Gamma(m_1)} K_{m_1}\big(2\sqrt{a_1}\big) + \frac{2m_2}{m_1+m_2} \frac{t^{\theta} a_2^{m_2/2}}{\Gamma(m_2)} K_{m_2}\big(2\sqrt{a_2}\big) \\ & + \frac{(m_1+m_2) t^{-\theta}}{\Gamma(m_1)\Gamma(m_2)} \int_0^{\infty} \int_0^{\infty} \frac{W^{m_1-1} M^{m_2-1} e^{-(W+M)}}{m_1 \exp(-a_1/W) + m_2 \exp(-a_2/M)}\, dM\, dW \\ & - \frac{m_1}{m_1+m_2} \frac{t^{\theta}}{\Gamma(m_1)} \int_{r_1'}^{r_2'} W^{m_1-1} \exp\Big( -W - \frac{a_1}{W} \Big)\, dW \\ & - \frac{m_2}{m_1+m_2} \Big[ I(r_2', m_1) - I(r_1', m_1) \Big] \frac{2\, t^{\theta} a_2^{m_2/2}}{\Gamma(m_2)} K_{m_2}\big(2\sqrt{a_2}\big) \\ & - \frac{(m_1+m_2) t^{-\theta}}{\Gamma(m_1)\Gamma(m_2)} \int_{r_1'}^{r_2'} \int_0^{\infty} \frac{W^{m_1-1} M^{m_2-1} e^{-(W+M)}}{m_1 \exp(-a_1/W) + m_2 \exp(-a_2/M)}\, dM\, dW. \end{aligned} \tag{48}$$

For $\tilde{R}_{\text{dsh2}}$, the expression is identical with $k_1$ replaced by $k_2 = \alpha^2$:

$$\mathcal{R}(\tilde{R}_{\text{dsh2}} \mid \text{PLF}) = \mathcal{R}(\tilde{R}_{\text{dsh1}} \mid \text{PLF})\big|_{k_1 \to k_2}. \tag{49}$$

**PLF-Risk of $\tilde{R}_{\text{dsh3}}$**

For $\tilde{R}_{\text{dsh3}}$, on $\mathcal{C}^{\star}$ the shrinkage weight becomes

$$k_3 = \frac{\tau}{r_1 + r_2} = \frac{2\lambda W}{r_1 + r_2}. \tag{50}$$

Thus, the $\mathcal{C}$-integrand in (42) takes the explicit form

$$t^{\theta} \Big( k_3 e^{-a_1/W} + (1-k_3) t^{-\lambda\theta} \Big) + \frac{t^{-\theta}}{k_3 e^{-a_1/W} + (1-k_3) t^{-\lambda\theta}} - 2,$$

and the $\mathcal{C}$-part becomes a $W$-integral over $(r_1', r_2')$. Combining this with the full pooled risk term and subtracting its $\mathcal{C}$-portion, and simplifying, yields the following closed form:

$$\begin{aligned}\mathcal{R}(\tilde{R}_{\text{dsh3}} \mid \text{PLF}) = \frac{1}{\Gamma(m_1)} \int_{r_1'}^{r_2'} \Bigg[ & \frac{2\lambda W}{r_1+r_2}\, t^{\theta} \exp\Big( -\frac{a_1}{W} \Big) + \Big( 1 - \frac{2\lambda W}{r_1+r_2} \Big) t^{-(\lambda-1)\theta} \\ & + \frac{t^{-\theta}}{\Big(\frac{2\lambda W}{r_1+r_2}\Big) \exp(-a_1/W) + \Big(1 - \frac{2\lambda W}{r_1+r_2}\Big) t^{-\lambda\theta}} - 2 \Bigg] W^{m_1-1} e^{-W}\, dW \\ & + \frac{2m_1}{m_1+m_2} \frac{t^{\theta} a_1^{m_1/2}}{\Gamma(m_1)} K_{m_1}\big(2\sqrt{a_1}\big) + \frac{2m_2}{m_1+m_2} \frac{t^{\theta} a_2^{m_2/2}}{\Gamma(m_2)} K_{m_2}\big(2\sqrt{a_2}\big) \\ & + \frac{(m_1+m_2) t^{-\theta}}{\Gamma(m_1)\Gamma(m_2)} \int_0^{\infty} \int_0^{\infty} \frac{W^{m_1-1} M^{m_2-1} e^{-(W+M)}}{m_1 \exp(-a_1/W) + m_2 \exp(-a_2/M)}\, dM\, dW \\ & - \frac{m_1}{m_1+m_2} \frac{t^{\theta}}{\Gamma(m_1)} \int_{r_1'}^{r_2'} W^{m_1-1} \exp\Big( -W - \frac{a_1}{W} \Big)\, dW \\ & - \frac{m_2}{m_1+m_2} \Big[ I(r_2', m_1) - I(r_1', m_1) \Big] \frac{2\, t^{\theta} a_2^{m_2/2}}{\Gamma(m_2)} K_{m_2}\big(2\sqrt{a_2}\big) \\ & - \frac{(m_1+m_2) t^{-\theta}}{\Gamma(m_1)\Gamma(m_2)} \int_{r_1'}^{r_2'} \int_0^{\infty} \frac{W^{m_1-1} M^{m_2-1} e^{-(W+M)}}{m_1 \exp(-a_1/W) + m_2 \exp(-a_2/M)}\, dM\, dW. \end{aligned} \tag{51}$$

**PLF-risk of $\tilde{R}_{\text{dsh4}}$**

For $\tilde{R}_{\text{dsh4}}$, on $\mathcal{C}^\star$ we have

$$k_4 = k_3^2 = \Big(\frac{2\lambda W}{r_1 + r_2}\Big)^2, \tag{52}$$

so the $\mathcal{C}$-integrand in (42) becomes

$$t^\theta\Big(k_4 e^{-a_1/W} + (1-k_4)t^{-\lambda\theta}\Big) + \frac{t^{-\theta}}{k_4 e^{-a_1/W} + (1-k_4)t^{-\lambda\theta}} - 2.$$

Combining the $\mathcal{C}$-term with the full pooled risk and subtracting its $\mathcal{C}$-portion, and simplifying, yields the closed form below:

$$\begin{aligned}
\mathcal{R}(\tilde{R}_{\text{dsh4}} \mid \text{PLF}) = \frac{1}{\Gamma(m_1)} \int_{r_1'}^{r_2'} \Bigg[ & \Big(\frac{2\lambda W}{r_1+r_2}\Big)^2 t^\theta \exp\Big(-\frac{a_1}{W}\Big) + \left(1 - \Big(\frac{2\lambda W}{r_1+r_2}\Big)^2\right) t^{-(\lambda-1)\theta} \\
& + \frac{t^{-\theta}}{\Big(\frac{2\lambda W}{r_1+r_2}\Big)^2 \exp(-a_1/W) + \left(1 - \Big(\frac{2\lambda W}{r_1+r_2}\Big)^2\right) t^{-\lambda\theta}} - 2 \Bigg] W^{m_1-1} e^{-W}\, dW \\
& + \frac{2m_1}{m_1+m_2} \frac{t^\theta a_1^{m_1/2}}{\Gamma(m_1)} K_{m_1}\big(2\sqrt{a_1}\big) + \frac{2m_2}{m_1+m_2} \frac{t^\theta a_2^{m_2/2}}{\Gamma(m_2)} K_{m_2}\big(2\sqrt{a_2}\big) \\
& + \frac{(m_1+m_2)t^{-\theta}}{\Gamma(m_1)\Gamma(m_2)} \int_0^\infty \int_0^\infty \frac{W^{m_1-1} M^{m_2-1} e^{-(W+M)}}{m_1 \exp(-a_1/W) + m_2 \exp(-a_2/M)}\, dM\, dW \\
& - \frac{m_1}{m_1+m_2} \frac{t^\theta}{\Gamma(m_1)} \int_{r_1'}^{r_2'} W^{m_1-1} \exp\Big(-W - \frac{a_1}{W}\Big)\, dW \\
& - \frac{m_2}{m_1+m_2} \Big[I(r_2', m_1) - I(r_1', m_1)\Big] \frac{2\, t^\theta a_2^{m_2/2}}{\Gamma(m_2)} K_{m_2}\big(2\sqrt{a_2}\big) \\
& - \frac{(m_1+m_2)t^{-\theta}}{\Gamma(m_1)\Gamma(m_2)} \int_{r_1'}^{r_2'} \int_0^\infty \frac{W^{m_1-1} M^{m_2-1} e^{-(W+M)}}{m_1 \exp(-a_1/W) + m_2 \exp(-a_2/M)}\, dM\, dW.
\end{aligned} \tag{53}$$

The relative risks under PLF are defined by

$$\begin{aligned}
RR_1 &= \frac{\mathcal{R}(\tilde{R}_{cd} \mid \text{PLF})}{\mathcal{R}(\tilde{R}_{\text{dsh1}} \mid \text{PLF})}, \qquad RR_2 = \frac{\mathcal{R}(\tilde{R}_{cd} \mid \text{PLF})}{\mathcal{R}(\tilde{R}_{\text{dsh2}} \mid \text{PLF})}, \\
RR_3 &= \frac{\mathcal{R}(\tilde{R}_{cd} \mid \text{PLF})}{\mathcal{R}(\tilde{R}_{\text{dsh3}} \mid \text{PLF})}, \qquad RR_4 = \frac{\mathcal{R}(\tilde{R}_{cd} \mid \text{PLF})}{\mathcal{R}(\tilde{R}_{\text{dsh4}} \mid \text{PLF})}.
\end{aligned} \tag{54}$$

Values $RR_j > 1$ indicate that $\tilde{R}_{\text{dsh}j}$ achieves a smaller PLF-risk than the classical pooled estimator $\tilde{R}_{cd}$.

**Theorem 1** (PLF convexity bound and why the improvement peaks near $\lambda \approx 1$)**.** Let $R = R(t;\theta) > 0$ and define $\phi(z) = z + z^{-1} - 2$ for $z > 0$ [12, **?**], so that $L(\tilde{R}, R) = \phi(\tilde{R}/R)$ is the PLF loss. Then, for any $z > 0$ and any $k \in [0,1]$,

$$\phi\big((1-k) + kz\big) \le k\, \phi(z). \tag{55}$$

In particular, if $\lambda = \theta_0/\theta = 1$, so that $R_0 = R(t;\theta_0) = R(t;\theta) = R$, then on the acceptance event $\mathcal{C} = \{r_1 < \tau < r_2\}$ each proposed estimator satisfies

$$L\Big(\tilde{R}_{\text{dsh}j}, R\Big) \le k_j\, L(\hat{R}_1, R), \qquad j = 1,2,3,4, \tag{56}$$

where $k_1 \in (0,1)$, $k_2 = \alpha^2 \in (0,1)$, $k_3 = \tau/(r_1+r_2) \in (0,1)$ on $\mathcal{C}$, and $k_4 = k_3^2 \in (0,1)$ on $\mathcal{C}$. Hence, relative to the classical pooled rule, used when $\tau \notin \mathcal{C}$, the only difference in PLF-risk comes from the acceptance region. When $\lambda = 1$, the shrinkage target equals the true reliability and the PLF loss on $\mathcal{C}$ is reduced by the factor

$k_j$. This provides a theoretical explanation for the pronounced improvement region and the observed peak of the relative-risk curves near $\lambda \approx 1$ in the numerical results, consistent with the general principle that shrinkage-based risk reduction is strongest when the target is close to the truth [5, 8, 13].

*Proof.* The function $\phi$ is convex on $(0, \infty)$ since $\phi''(z) = 2z^{-3} > 0$. Therefore, by Jensen's inequality,

$$\phi\big((1-k)\cdot 1 + k\cdot z\big) \le (1-k)\phi(1) + k\phi(z),$$

since $\phi(1) = 1+1-2 = 0$, we obtain $(1-k)\phi(1)+k\phi(z) = k\phi(z)$, which gives (55). If $\lambda = 1$, then $R_0 = R$ and on $\mathcal{C}$ we have $\tilde{R}_{\text{dsh}j} = (1-k_j)R + k_j\hat{R}_1$, so applying (55) with $z = \hat{R}_1/R$ yields (56). The bounds $0 < k_3 < 1$ and $0 < k_4 < 1$ on $\mathcal{C}$ follow from $r_1 < \tau < r_2$ and $r_2 < r_1 + r_2$. □

**Remark 2.** The inequality $(z - z^*)^\top \phi(z) \le 0$ in the proof uses the fact that $-\phi$ is monotone decreasing, equivalently that $\phi$ is convex and $\phi'(z) = 1-z^{-2}$ is increasing, which is consistent with $\phi''(z) = 2z^{-3} > 0$. No confusion with the notion of a monotone mapping should arise: here $\phi$ denotes the scalar function $\phi(z) = z + z^{-1} - 2$, not a vector-valued mapping, and the stated convexity bound follows directly from Jensen's inequality as shown above.

## 4 Numerical Results

### 4.1 Numerical Evaluation Setting

**Computational setting.** All numerical values reported in this section are obtained by direct numerical evaluation of the derived analytical expressions, including one-dimensional and two-dimensional integrals and special functions, implemented in Python. No Monte Carlo simulation is used.

The comparison is conducted under the Precautionary Loss Function (PLF) using: (i) the bias ratio ($BR$), (ii) the PLF-risk, and (iii) the corresponding relative risk ($RR$) with respect to the classical pooled benchmark $\tilde{R}_{cd}$.

Unless stated otherwise, the study uses the grid

$$k_1 \in \{0.1, 0.5\}, \qquad (m_1, m_2) \in \{5, 10, 15\}^2, \qquad \alpha \in \{0.01, 0.05\},$$

$$\lambda = \theta_0/\theta \in \{0.2, 0.4, \ldots, 1.8\}, \qquad \beta = R(t;\theta) = t^{-\theta} \in \{0.3, 0.6, 0.9\}.$$

### 4.2 Main Numerical Findings

Across all four proposed estimators, the relative-risk curves exhibit a pronounced improvement region when $\lambda = \theta_0/\theta$ is close to one. In this neighborhood, the prior target $\theta_0$ is close to the true value of $\theta$, so the shrinkage component reduces the PLF-risk, which is reflected by $RR > 1$. As $\lambda$ departs from one, that is, under prior misspecification, the advantage diminishes and the relative risk decreases accordingly.

The stage sample sizes also have a systematic effect. Increasing $(m_1, m_2)$ yields smoother and more stable relative-risk profiles and reduces extreme behavior under larger departures from $\lambda \approx 1$. Likewise, the bias ratio is closest to zero near $\lambda \approx 1$, while $|BR|$ increases gradually as $\lambda$ moves away from one. This pattern is expected: shrinkage introduces little distortion when $\theta_0$ is credible, whereas misspecification induces additional bias. Importantly, the increase in $|BR|$ is structured and becomes smaller for larger values of $(m_1, m_2)$.

Changing the test level from $\alpha = 0.01$ to $\alpha = 0.05$ mainly affects the magnitude, that is, the height and width, of the improvement region, while preserving the same qualitative relative-risk profile. The tuning parameter $k_1$

controls the risk-bias trade-off in the shrinkage component: different values of $k_1$ alter the strength of shrinkage toward $R_0$ and hence modify both the height of the relative-risk peak near $\lambda \approx 1$ and the bias magnitude when $\lambda$ is far from one. The numerical evidence also indicates that the preferred estimator may vary with the reliability level $\beta$, so practical recommendations should be interpreted jointly with the target reliability setting. Overall, the strongest gains are obtained when the prior information is credible, whereas larger deviations from $\lambda = 1$ reduce the risk advantage and increase sensitivity to the shrinkage choice.

### 4.3 Real-Data Illustration

To illustrate the practical implementation of the proposed estimators, we consider an observed dataset under a progressively Type-II censoring plan. This illustration is a direct application of the decision rule and the shrinkage weights; it is not a Monte Carlo study.

*Dataset and censoring plan.* We extract a subset of positive observations from the *Public Health Infobase – Data on COVID-19 in Canada*, an openly available time-series dataset published by the Public Health Agency of Canada [16]. The selected observations are used here solely to demonstrate the computational steps of the proposed estimators under a progressively Type-II censoring plan applied to a real dataset; this subsection is not intended as a formal goodness-of-fit analysis for the Pareto model. A progressively Type-II right censoring scheme with total size $n = 25$ and observed failures $m = 15$ is then imposed, split into two independent stages with $(m_1, m_2) = (10, 5)$.

*Stage MLEs and prior target.* Using the stage-wise MLEs, we obtain $\hat{\theta}_1 = 0.457099$ and $\hat{\theta}_2 = 0.826312$. We take the prior target as $\theta_0 = 0.537094$, so that $R_0(t) = t^{-\theta_0}$.

*Preliminary test decision.* With $\tau = 2m_1\theta_0/\hat{\theta}_1$, we obtain $\tau \approx 23.5001$. For $\alpha = 0.01$, $(r_1, r_2) = (7.433844,\ 39.996846)$, hence $\tau \in (r_1, r_2)$ and $H_0$ is accepted. Therefore, the proposed estimators shrink toward $R_0(t)$ and are given by

$$\tilde{R}_{\text{dsh1}}(t) = k_1\hat{R}_1(t) + (1-k_1)R_0(t), \qquad \tilde{R}_{\text{dsh2}}(t) = k_2\hat{R}_1(t) + (1-k_2)R_0(t),$$

$$\tilde{R}_{\text{dsh3}}(t) = k_3\hat{R}_1(t) + (1-k_3)R_0(t), \qquad k_3 = \frac{\tau}{r_1+r_2},$$

$$\tilde{R}_{\text{dsh4}}(t) = k_4\hat{R}_1(t) + (1-k_4)R_0(t), \qquad k_4 = k_3^2,$$

where $\hat{R}_i(t) = t^{-\hat{\theta}_i}$, for $i = 1, 2$, and $k_2 = \alpha^2 = 10^{-4}$. The classical pooled benchmark is

$$\tilde{R}_{cd}(t) = \frac{m_1\hat{R}_1(t) + m_2\hat{R}_2(t)}{m_1+m_2}.$$

Numerically, $k_3 \approx 0.4955$ and $k_4 \approx 0.2455$.

*Comparison across multiple mission times.* Table 2 reports the resulting reliability estimates for several mission times $t$, illustrating how the final estimator changes with $t$ while the test decision and weights remain fixed.

### 4.4 Optimal Design Parameter Interpretation

The closed-form PLF-risk expressions derived in Section 3 also allow the numerical results to be interpreted from a design-optimization perspective. In particular, once the estimator form is fixed, the choice of the design parameters $(k_1, \alpha, m_1, m_2)$ determines the resulting PLF-risk profile over the prior ratio $\lambda = \theta_0/\theta$. Hence, the numerical

**Table 2:** Real-data illustration: estimates at multiple mission times ($m_1 = 10, m_2 = 5, \alpha = 0.01$; $k_2 = \alpha^2$; $k_3 = \tau/(r_1+r_2)$; $k_4 = k_3^2$).

| $t$ | $\tilde{R}_{cd}(t)$ | $\tilde{R}_{\text{dsh1}}(t)$ $(k_1 = 0.1)$ | $\tilde{R}_{\text{dsh1}}(t)$ $(k_1 = 0.5)$ | $\tilde{R}_{\text{dsh2}}(t)$ | $\tilde{R}_{\text{dsh3}}(t)$ | $\tilde{R}_{\text{dsh4}}(t)$ |
|---|---|---|---|---|---|---|
| 2 | 0.6912 | 0.7285 | 0.7319 | 0.7329 | 0.7319 | 0.7347 |
| 3 | 0.5379 | 0.5591 | 0.5794 | 0.5617 | 0.5793 | 0.5656 |
| 5 | 0.3832 | 0.3953 | 0.4091 | 0.3960 | 0.4090 | 0.4000 |

evaluation carried out on the design grid may be viewed as a systematic search for configurations that achieve favorable risk performance under prior uncertainty.

From this perspective, the relative-risk results reported in Appendix A provide direct guidance on how to select the shrinkage weight, significance level, and stage sample sizes so as to improve performance relative to the classical pooled estimator. For example, the numerical findings show that the most favorable configurations are typically those producing the strongest and most stable improvement region around $\lambda \approx 1$, while also controlling the deterioration in risk when the prior information is misspecified. Thus, the design problem is not merely to maximize improvement at a single value of $\lambda$, but rather to balance local gains near the prior target against robustness over a wider range of plausible prior ratios.

Accordingly, the present numerical study may be interpreted as a constrained optimization exercise under uncertainty: among admissible values of $(k_1, \alpha, m_1, m_2)$, one seeks designs that minimize the PLF-risk, or equivalently maximize relative-risk performance, over a practically relevant range of $\lambda$. A formal minimax formulation may be considered as a natural extension of the present framework.

### 4.5 Graphical Analysis of PLF-Risk and Bias-Ratio Behavior

The following figures provide the retained graphical summaries of the numerical study. They display the relative-risk and bias-ratio behavior of the proposed estimators under the Precautionary Loss Function (PLF) across the design settings considered in this paper.

**Relative-Risk Figures**

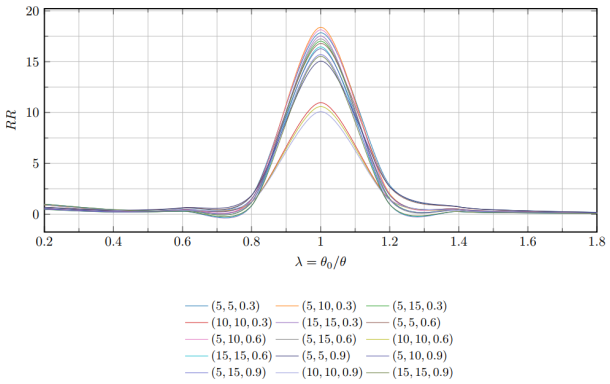


**Figure 1:** PLF relative-risk curves $RR(\tilde{R}_{\text{dsh1}})$ for $k_1 = 0.1$ and $\alpha = 0.01$. The largest improvement occurs near $\lambda \approx 1$, where the prior target is well aligned with the true parameter value.

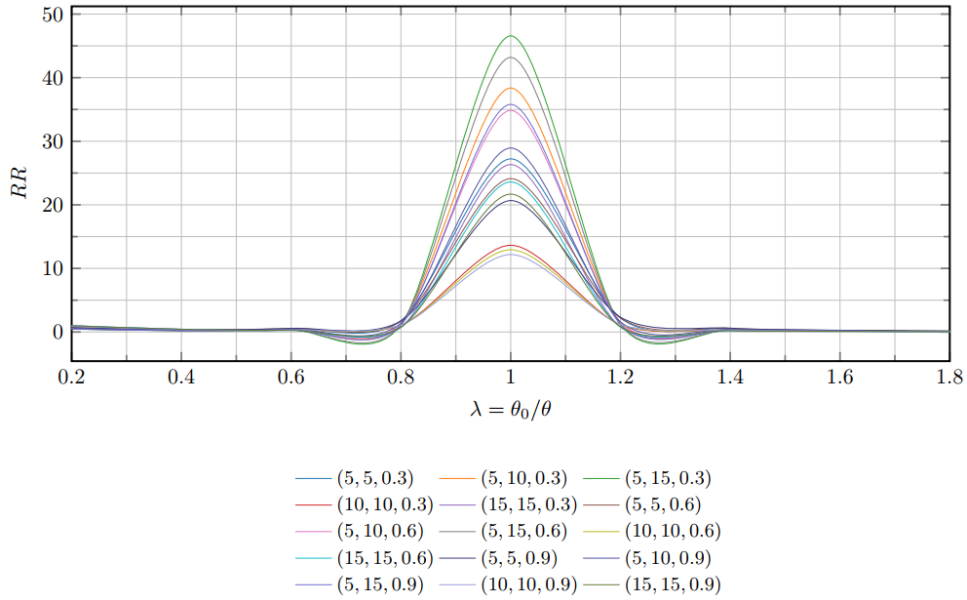


**Figure 2:** Representative PLF relative-risk curves $RR(\tilde{R}_{\text{dsh2}})$ for $\alpha = 0.01$.

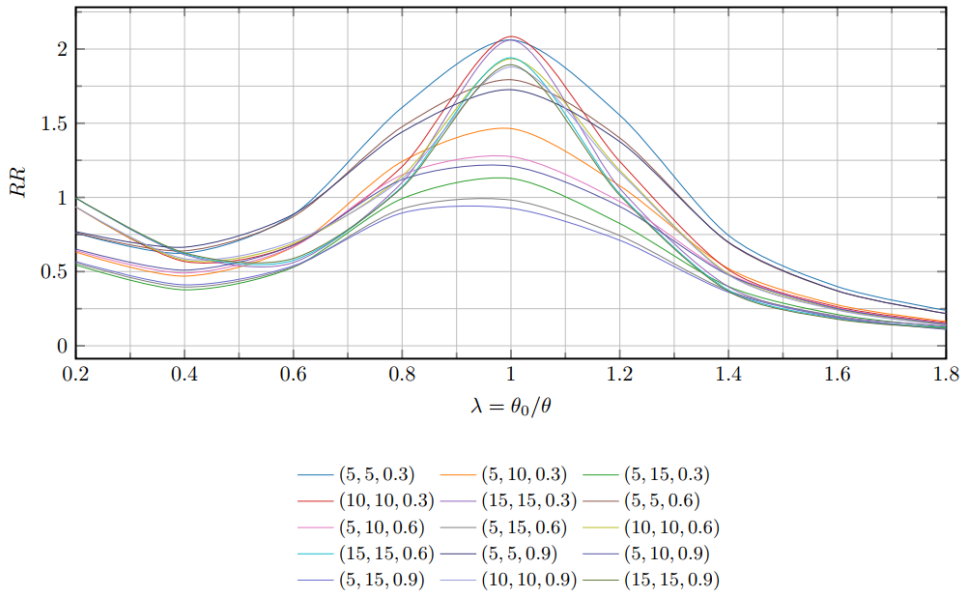


**Figure 3:** Representative PLF relative-risk curves $RR(\tilde{R}_{\text{dsh3}})$ for $\alpha = 0.01$.

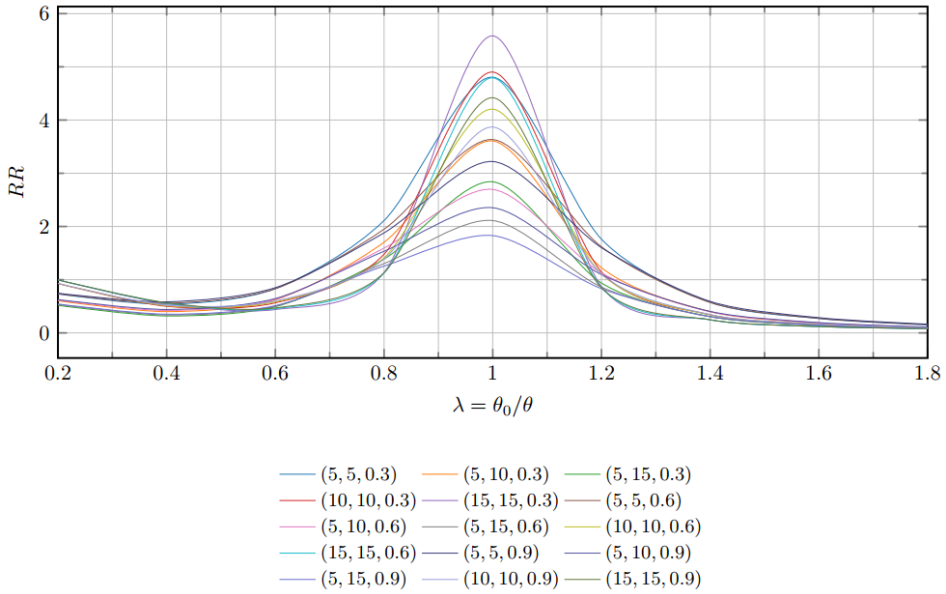


**Figure 4:** Representative PLF relative-risk curves $RR(\tilde{R}_{\text{dsh4}})$ for $\alpha = 0.01$.

**Bias-Ratio Figures**

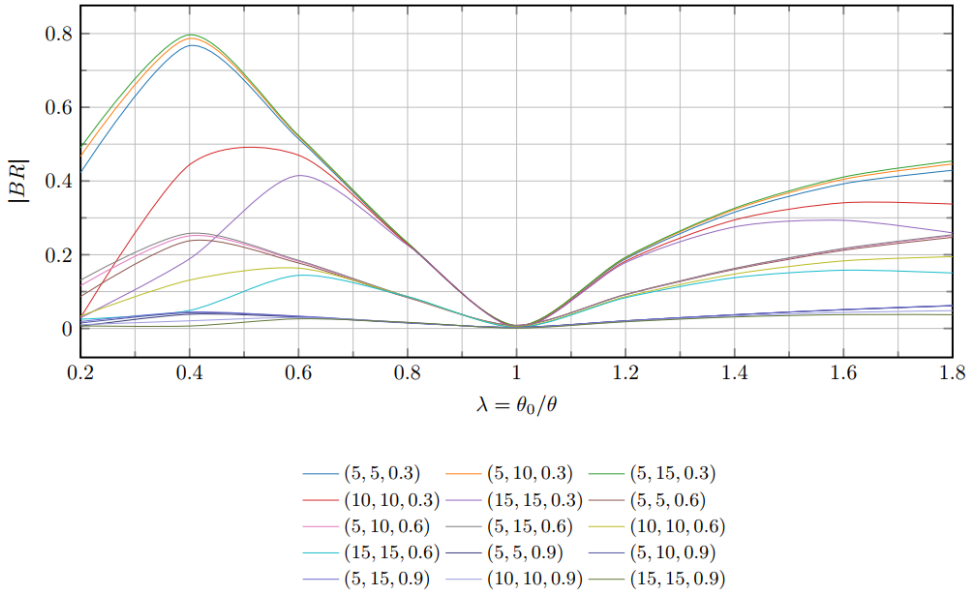


**Figure 5:** Absolute bias-ratio curves $|BR(\tilde{R}_{\text{dsh1}})|$ for $\alpha = 0.01$ and $k_1 = 0.1$.

### 4.6 Tabular Summary of Key Numerical Findings

This section presents the retained representative numerical tables for the proposed double pre-test shrinkage estimators under the Precautionary Loss Function (PLF). To avoid redundancy, only a limited number of tables are reported here for direct numerical reference, while the corresponding graphical summaries are presented in Section 4.5. The retained tables summarize the main numerical patterns of the relative-risk and bias-ratio measures over the considered prior-ratio grid.

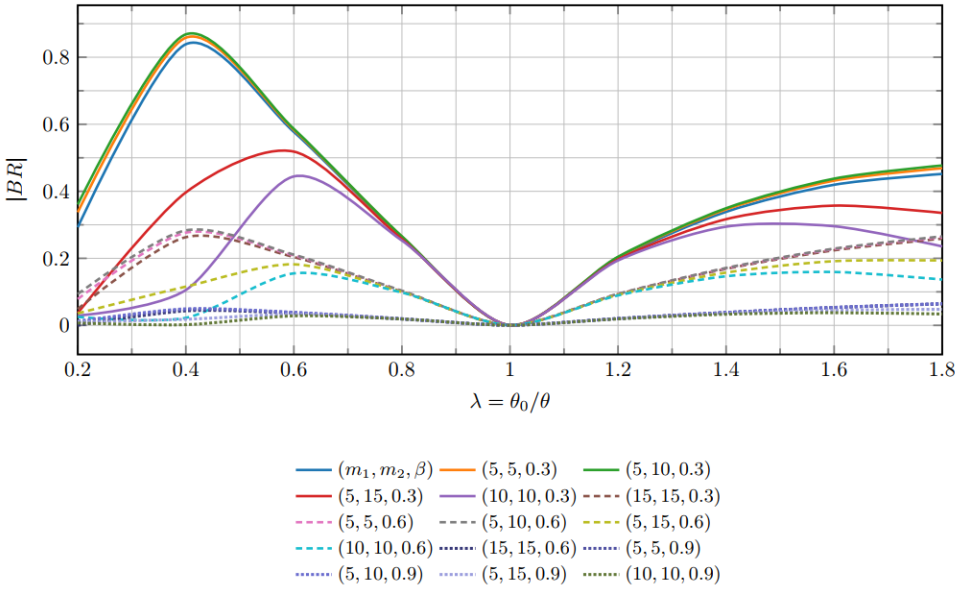


**Figure 6:** Absolute bias-ratio curves $|BR(\tilde{R}_{\text{dsh2}})|$ under PLF for $\alpha = 0.01$.

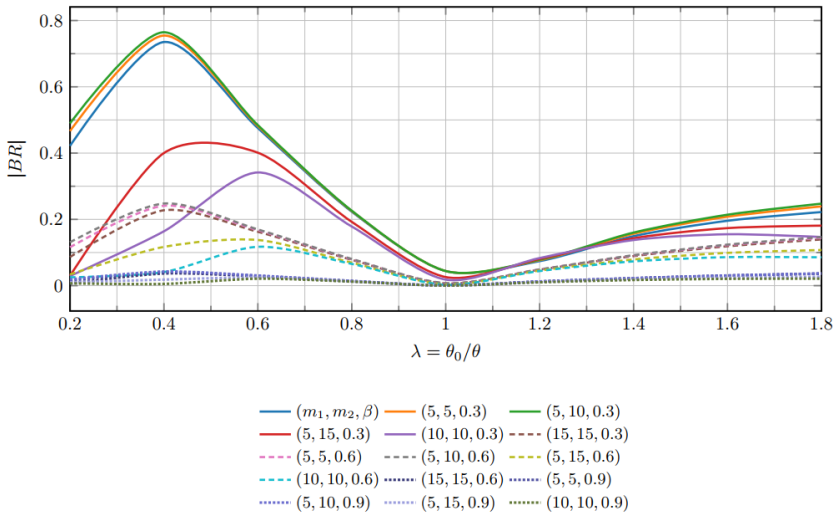


**Figure 7:** Absolute bias-ratio curves $|BR(\tilde{R}_{\text{dsh3}})|$ under PLF for $\alpha = 0.01$.

Table 3 reports representative numerical values of the PLF relative risk for $\tilde{R}_{\text{dsh1}}$ under selected configurations. Table 4 reports the corresponding representative numerical values of the absolute bias ratio. Together, these tables provide direct numerical support for the main graphical findings and confirm that the strongest improvement typically occurs near $\lambda \approx 1$.

**Table 3:** Representative numerical values of the PLF relative risk $RR(\tilde{R}_{\text{dsh1}})$ for $k_1 = 0.1$ and $\alpha = 0.01$.

| $m_1$ | $m_2$ | $\beta$ | $\lambda = 0.2$ | $\lambda = 0.4$ | $\lambda = 0.6$ | $\lambda = 0.8$ | $\lambda = 1.0$ | $\lambda = 1.2$ | $\lambda = 1.4$ | $\lambda = 1.6$ | $\lambda = 1.8$ |
|---|---|---|---|---|---|---|---|---|---|---|---|
| 5 | 5 | 0.3 | 0.6776 | 0.3666 | 0.6012 | 1.8457 | 17.8403 | 2.8553 | 0.7398 | 0.3437 | 0.1979 |
| 10 | 10 | 0.3 | 0.9069 | 0.3925 | 0.3583 | 1.2040 | 10.9731 | 1.4616 | 0.3846 | 0.1837 | 0.1070 |
| 15 | 15 | 0.3 | 0.9952 | 0.4443 | 0.2836 | 0.8359 | 17.5228 | 0.9895 | 0.2626 | 0.1277 | 0.0856 |
| 5 | 5 | 0.6 | 0.6859 | 0.3791 | 0.6141 | 1.8394 | 16.7969 | 2.6976 | 0.7140 | 0.3297 | 0.1888 |
| 10 | 10 | 0.6 | 0.9096 | 0.4019 | 0.3674 | 1.2186 | 10.5914 | 1.4227 | 0.3762 | 0.1806 | 0.1046 |
| 15 | 15 | 0.6 | 0.9953 | 0.4530 | 0.2902 | 0.8430 | 16.4578 | 0.9703 | 0.2576 | 0.1257 | 0.0851 |
| 5 | 5 | 0.9 | 0.6976 | 0.3979 | 0.6421 | 1.8657 | 15.0503 | 2.7126 | 0.7328 | 0.3375 | 0.1925 |
| 10 | 10 | 0.9 | 0.9113 | 0.4107 | 0.3787 | 1.2464 | 10.0902 | 1.4310 | 0.3796 | 0.1823 | 0.1050 |
| 15 | 15 | 0.9 | 0.9953 | 0.4590 | 0.2969 | 0.8561 | 15.5316 | 0.9734 | 0.2582 | 0.1259 | 0.0852 |

**Table 4:** Representative numerical values of the absolute bias ratio $|BR(\tilde{R}_{\text{dsh1}})|$ for $k_1 = 0.1$ and $\alpha = 0.01$.

| $m_1$ | $m_2$ | $\beta$ | $\lambda = 0.2$ | $\lambda = 0.4$ | $\lambda = 0.6$ | $\lambda = 0.8$ | $\lambda = 1.0$ | $\lambda = 1.2$ | $\lambda = 1.4$ | $\lambda = 1.6$ | $\lambda = 1.8$ |
|---|---|---|---|---|---|---|---|---|---|---|---|
| 5 | 5 | 0.3 | 0.422476 | 0.767168 | 0.514317 | 0.229498 | 0.007410 | 0.188740 | 0.315402 | 0.392478 | 0.429002 |
| 10 | 10 | 0.3 | 0.029051 | 0.444136 | 0.469993 | 0.228507 | 0.004404 | 0.182661 | 0.294399 | 0.340887 | 0.337416 |
| 15 | 15 | 0.3 | 0.029096 | 0.188883 | 0.414622 | 0.225980 | 0.003144 | 0.178720 | 0.275443 | 0.293298 | 0.259234 |
| 5 | 5 | 0.6 | 0.086480 | 0.237695 | 0.177486 | 0.083692 | 0.008786 | 0.091578 | 0.160204 | 0.212128 | 0.247224 |
| 10 | 10 | 0.6 | 0.033791 | 0.131144 | 0.163517 | 0.086200 | 0.004643 | 0.086124 | 0.147637 | 0.183349 | 0.194680 |
| 15 | 15 | 0.6 | 0.025262 | 0.048905 | 0.144073 | 0.086227 | 0.003136 | 0.083477 | 0.137740 | 0.157976 | 0.150414 |
| 5 | 5 | 0.9 | 0.006090 | 0.038483 | 0.031029 | 0.014833 | 0.003123 | 0.020845 | 0.037065 | 0.050801 | 0.061527 |
| 10 | 10 | 0.9 | 0.010109 | 0.020773 | 0.029562 | 0.016340 | 0.001418 | 0.018943 | 0.033616 | 0.043520 | 0.048209 |
| 15 | 15 | 0.9 | 0.007013 | 0.006616 | 0.026158 | 0.016586 | 0.000914 | 0.018219 | 0.031280 | 0.037490 | 0.037299 |

### 4.7 Computational Procedure

This section summarizes how the numerical results reported in the paper were obtained. All values of the bias ratio, PLF-risk, and relative risk were computed by direct numerical evaluation of the analytical expressions derived in Section 3, rather than by Monte Carlo simulation. For each selected configuration of $(m_1, m_2)$, $\alpha$, $\beta$, and $\lambda = \theta_0/\theta$, we first evaluated the required incomplete-gamma and modified Bessel-function components, together with the one-dimensional and two-dimensional integrals appearing in the closed-form formulas. These quantities were then substituted into the expressions of $(\tilde{R}_{\text{dsh}j})$, $\mathcal{R}(\tilde{R}_{\text{dsh}j} \mid \text{PLF})$, and $RR_j$, for $j = 1, 2, 3, 4$. The full numerical study was implemented in Python, and the resulting values were used directly to generate the tables and figures reported in Sections 4.5 and 4.6. This computational strategy ensures exact consistency between the theoretical formulas and the reported numerical results.

## 5 Conclusion

This paper introduced a class of double pre-test shrinkage estimators for the reliability function of the Pareto distribution under progressive Type-II censoring and evaluated their performance under the Precautionary Loss Function (PLF). The proposed framework combines a preliminary test on the shape parameter with shrinkage toward a prior target value, yielding four reliability estimators with fixed and data-dependent shrinkage weights.

The central analytical contribution is the derivation of closed-form expressions for the bias, bias ratio, PLF-risk, and relative risk of the proposed estimators. These expressions enable direct comparisons with the classical pooled estimator and illuminate how the shrinkage weight, significance level, stage sample sizes, and prior ratio jointly determine estimator performance. In particular, the theoretical analysis reveals that the greatest gains arise when the prior target is close to the true parameter value—an insight that accounts for the improvement region observed numerically in the vicinity of $\lambda \approx 1$.

The numerical study confirmed that the proposed estimators can achieve substantial PLF-risk reductions relative to the classical pooled estimator across a wide range of design configurations. The results further indicate that no single estimator dominates uniformly across all settings. Fixed-weight shrinkage tends to yield stronger gains when prior information is reliable, while adaptive shrinkage offers greater stability under prior misspecification. Together, these estimators form a flexible family that can be tailored to the intended balance between risk reduction and robustness.

From an optimization standpoint, the estimation problem can be naturally recast as the minimization of PLF-risk over admissible design choices. In this interpretation, the shrinkage weight, significance level, and stage sample sizes function as decision variables that govern estimation performance, situating the present methodology within a broader optimization-oriented framework for decision-making under uncertainty.

Several limitations of this study merit acknowledgment. The performance gains of the proposed estimators depend on the proximity of the prior target to the true parameter value, and their advantage diminishes when prior information is substantially misspecified. The analysis is also currently confined to the Pareto distribution, progressive Type-II censoring, and the PLF criterion.

Future research may extend the proposed framework to other lifetime distributions, alternative censoring schemes, and additional asymmetric loss functions. Further directions of interest include developing data-driven selection rules for the shrinkage parameters and exploring Bayesian and empirical Bayes extensions of the present methodology.

## Declarations

### Availability of Supporting Data

All data generated or analyzed during this study are included in this published paper.

### Funding

The authors conducted this research without any funding, grants, or support.

### Conflict of Interest

The authors declare that they have no known competing financial interests or personal relationships that could have influenced the work reported in this paper.

### Author Contributions

**Omar J. A. Al-Qaragholi** contributed to conceptualization, methodology, formal analysis, software implementation, data curation, writing of the original draft, and preparation of the numerical results. **Alaa Khlaif**

**Jiheel** contributed to supervision, validation, review and editing of the manuscript, and the overall scientific guidance of the study. All authors read and approved the final manuscript.

**Artificial Intelligence Statement**

Artificial intelligence (AI) tools, including large language models, were used solely for language editing and improving readability. AI tools were not used for generating ideas, performing analyses, interpreting results, or writing the scientific content. All scientific conclusions and intellectual contributions were made exclusively by the authors.

**Publisher's Note**

The publisher remains neutral regarding jurisdictional claims in published maps and institutional affiliations.

## References

[1] Abd Ali, M.H., Jiheel, A.K., Al-Hemyari, Z. (2022). "Two-stage shrinkage Bayesian estimators for the shape parameter of Pareto distribution dependent on Katti's regions". *Iraqi Journal for Computer Science and Mathematics*, 3(2), 42–54. https://doi.org/10.52866/ijcsm.2022.02.01.005

[2] Aghamohammadi, S. Z. (2026). "On double-stage Bayesian Shrinkage estimator for two-parameter exponential distribution under progressively type-II censored data". *Journal of Statistical Computation and Simulation*, 1–19. https://doi.org/10.1080/00949655.2025.2612260

[3] Al-Bayyati, H. A., Arnold, J.C. (1972). "On double-stage estimation in simple linear regression using prior knowledge". *Technometrics*, 14(2), 405–414. https://doi.org/10.1080/00401706.1972.10488925

[4] Arnold, B.C. (1983). *Pareto Distributions*. International Cooperative Publishing House, Fairland, MD.

[5] Atewi, I.J., Jiheel, A.K., Shanubhogue, A.R.R. (2023). "Double-stage shrinkage estimation of reliability function for Burr XII distribution". *Iraqi Journal for Computer Science and Mathematics*, 4(1), 35–52. https://doi.org/10.52866/ijcsm.2023.01.01.005

[6] Balakrishnan, N., Aggarwala, R. (2000). *Progressive censoring: Theory, methods, and applications*. Birkhäuser Boston, MA. https://doi.org/10.1007/978-1-4612-1334-5

[7] Balakrishnan, N., Cramer, E. (2014). *The art of progressive censoring: Applications to reliability and quality*. Birkhäuser New York, NY. https://doi.org/10.1007/978-0-8176-4807-7

[8] Chiou, P. (2007). "Shrinkage estimation of reliability in the exponential distribution". *Communications in Statistics – Theory and Methods*, 21(6), 1745–1758. https://doi.org/10.1080/03610929208830876

[9] Gupta, R., Bhougal, S., Joorel, J.P.S. (2006). "A two-stage procedure for estimation of the common mean of several normal populations having unequal and unknown variances". *Model Assisted Statistics and Applications*. https://doi.org/10.3233/MAS-2006-1401

[10] Jiheel, A.K., Al-Qatifi, A.B.J. (2020). "Bayes pre-test shrinkage estimation of Rayleigh distribution under different loss functions". *International Journal of Advances in Applied Mathematics and Mechanics*, 7(4), 72–90. https://www.ijaamm.com/uploads/2/1/4/8/21481830/v7n4p7_72-90.pdf

[11] Kumar, I., Kumar, K. (2022). "On estimation of $P(V < U)$ for inverse Pareto distribution under progressively censored data". *International Journal of System Assurance Engineering and Management*, 13, 189–202. https://doi.org/10.1007/s13198-021-01193-w

[12] Norström, J.G. (1996). "The use of the precautionary loss function in risk analysis". *IEEE Transactions on Reliability*, 45(3), 400–403. https://doi.org/10.1109/24.536992

[13] Sabr, M.R., Jiheel, A.K. (2024). "Pre-test shrinkage estimation for reliability function of Burr XII distribution using progressive Type II censored sample under precautionary loss function (PLF)". *Journal of Education for Pure Science*, 14(3). https://doi.org/10.32792/jeps.v14i3.549

[14] Thompson, J.R. (1968). "Some shrinkage techniques for estimating the mean". *Journal of the American Statistical Association*, 63(321), 113–122. https://doi.org/10.1080/01621459.1968.11009226

[15] Ye, Z., Gui, W. (2024). "Estimation and Bayesian prediction of the generalized Pareto distribution based on progressively Type-II censored samples". *Applied Sciences*, 14(18), 8433. https://doi.org/10.3390/app14188433

[16] Public Health Agency of Canada (PHAC). (2020–2023). *Public Health Infobase – Data on COVID-19 in Canada*. Government of Canada Open Data Portal. Dataset ID: 261c32ab-4cfd-4f81-9dea-7b64065690dc. (Accessed: 2024). https://open.canada.ca/data/en/dataset/261c32ab-4cfd-4f81-9dea-7b64065690dc

**Authors Bio-sketches**

**Omar J. A. Al-Qaragholi** is an affiliate of the Department of Mathematics, College of Education for Pure Sciences, University of Thi-Qar, Nasiriyah, Iraq. His scholarly interests span mathematical statistics, reliability analysis, shrinkage estimation, censoring schemes, and applied probability. Corresponding author. Email: omar_jabar@utq.edu.iq

**Alaa Khlaif Jiheel** is an affiliate of the Department of Mathematics, College of Education for Pure Sciences, University of Thi-Qar, Nasiriyah, Iraq. His scholarly interests encompass mathematical statistics, statistical inference, reliability theory, and applied mathematics.